

**NANYANG
TECHNOLOGICAL
UNIVERSITY**

SINGAPORE

**Blemishes Change Simulation for
Facial Image Retouching via
Physics-Based Modelling**

SHUAI CHENHAO

SCHOOL OF ELECTRICAL AND ELECTRONIC ENGINEERING

2023

Blemishes Change Simulation for Facial Image Retouching via Physics-Based Modelling

SHUAI CHENHAO

SCHOOL OF ELECTRICAL AND ELECTRONIC ENGINEERING

**A DISSERTATION SUBMITTED IN PARTIAL FULFILMENT OF
THE REQUIREMENTS FOR THE DEGREE OF
MASTER OF SCIENCE IN SIGNAL PROCESSING**

2023

Statement of Originality

I hereby certify that the work embodied in this thesis is the result of original research and has not been submitted for a higher degree to any other University or Institution.

.....

Date

.....

Your Name

Supervisor Declaration Statement

I have reviewed the content and presentation style of this thesis and declare it is free of plagiarism and of sufficient grammatical clarity to be examined. To the best of my knowledge, the research and writing are those of the candidate except as acknowledged in the Author Attribution Statement. I confirm that the investigations were conducted in accord with the ethics policies and integrity standards of Nanyang Technological University and that the research data are presented honestly and without prejudice.

.....

Date

.....

Supervisor's Name

Authorship Attribution Statement

This thesis does not contain any materials from papers published in peer-reviewed journals or from papers accepted at conferences in which I am listed as an author.

.....

Date

.....

Your Name

Table of Contents

Abstract	iii
Acronyms	iv
Symbols	v
Lists of Figures	viii
Lists of Tables	ix
1 Introduction	1
1.1 Background	1
1.2 Motivation	2
1.3 Objectives and Specifications	3
1.4 Major contribution of the Dissertation	4
1.5 Organisation of the Dissertation	5
2 Literature Review	7
2.1 Skin Chromophores & Blemishes	7
2.2 Skin Modeling & Rendering Techniques	9
2.3 Controllable Facial Image Editing	12
2.3.1 Objectives and Definitions	12
2.3.2 Dataset and Stability	13
2.3.3 Controllability	14
3 Methods	16
3.1 Skin Chromophore Color Space Decomposition	16
3.2 Blemishes Appearance Modelling & Editing	19
3.2.1 Algorithm Implementations	21
4 Experiments	26
4.1 Dataset	26
4.2 Experiment Setup	28
4.2.1 Objective Evaluation	30
4.2.2 Subjective Evaluation	30

5 Result & Discussion	33
5.1 Versatility	34
5.2 Reality	35
5.3 Controllability	38
5.4 Perception Study	38
6 Conclusion	41
References	43
Appendix A Simulation on Various Skin Tones	49

Abstract

Facial image retouching aims to remove facial blemishes from images, such as acne and pigmentation, and still retain textures and details. Nevertheless, existing methods just completely remove the blemishes but focus little on realism of the intermediate process, limiting their use more to beautifying facial images on social media rather than being effective tools for simulating changes in facial pigmentation and acne to demonstrate the efficacy of skincare product to consumers or to assess the skincare product development. To bridge this critical gap, an efficient framework is proposed for simulating changes in skin blemishes. This method is based on prior knowledge that links the appearance of acne and pigmentation to melanin and hemoglobin chromophores under the skin surface. This novel framework models the spatial distributions of chromophores under the optical scattering properties of the skin. A unique feature of this framework is the precise and stable manipulation of parameters of chromophore distributions, thereby enabling control over the appearance of skin blemishes. The proposed framework is validated using a comprehensive dataset containing temporal data on long-term skin blemish changes. Experiment results show that this framework achieves highly realistic simulations. Furthermore, a visual perception study has also demonstrated the authenticity and quality of the proposed simulation method. Moreover, an user-friendly graphic interface is implemented to manipulate the facial blemishes interactively, achieving realistic and gradual blemishes retouching with an easy access.

Keywords: Facial Image Retouching, Computer Vision, Skin Image.

Acronyms

FID	Fréchet Inception Distance
GAN	Generative Adversarial Network
UV	Ultraviolet Light
sRGB	Standard RGB color space
LoRA	Low-Rank Adaption
BSSRDF	Bidirectional Surface Scattering Reflectance Distribution Function
ITA	Individual Typology Angle
PS	Adobe Photoshop
SD	Stable Diffusion

Symbols

A	Absorption
R	Reflection intensity
λ	Wavelengths
ε	Extinction coefficient of chromophore
C	Relative chromophore concentration
C_H	Relative concentration of heamoglobin
C_M	Relative concentration of melanin
C_r	Relative concentration of residual chromophore
l	Mean optical path length
l_H	Mean optical path length for heamoglobin
l_M	Mean optical path length for melanin
l_r	Mean optical path length for residual chromophore
ε_H	Extinction coefficient of heamoglobin
ε_M	Extinction coefficient of melanin
ε_r	Extinction coefficient of residual chromophore
$\mathcal{R}, \mathcal{G}, \mathcal{B}$	Red, Green, Blue camera pixel channels
\mathbf{E}	Matrix of extinction coefficients and path lengths
\mathbf{c}	Vector of chromophore concentrations
\mathbf{k}	Vector of reflection intensities for RGB channels
G	Gaussian function
μ	Mean (center) of a Gaussian distribution
σ	Standard deviation of a Gaussian distribution
a	Amplitude factor of a Gaussian distribution
Σ	Covariance matrix
\mathbf{R}	Rotation matrix
\mathbf{S}	Scaling matrix
θ	Rotation angle
α_K	Gain factor for chromophore K
C_K	Chromophore concentration for channel K
\hat{C}_K	Estimated chromophore concentration for channel K
C_K^{skin}	Chromophore concentration of normal skin for channel K
C_K^{blem}	Chromophore concentration of blemish for channel K
h, w	Height and width of an image patch
\mathbf{x}	Coordinate vector in the image plane
Θ	Overall parameters to be fitted

List of Figures

2.1	Spectral absorption coefficients of skin chromophore. This work focused on modelling haemoglobin and melanin distribution of skin blemishes. Image taken from [1]	8
2.2	Layered skin model. A portion of the incident light undergoes specular reflection, revealed as a skin texture layer. The other part transmits into and is scattered by the Epidermis and Dermis. Melanin and haemoglobin, which are distributed in these two layers, absorb specific wavelengths of light, rendering the skin's characteristic color.	10
3.1	An overview of the proposed skin blemish change simulation pipeline. In the pipeline, a box of Region of Interest (ROI) is first used to select the blemish like acne or pigmentation. Then, a <i>Layer Separation Filter</i> is applied to separate the texture layer and the diffusion layers. A <i>Sum-of-Gaussians</i> model is fitted to each ROI in <i>Melanin/Heamoglobin</i> color space, with the parameters of the fitted model adjusted to manipulate the appearance of the blemishes. The modified diffusion layer is summed with the original texture layer to obtain the output.	17
3.2	3D scatter plot showing the distribution of skin colors sampled from the face skin images in a dataset, illustrating the correlation between the R, G, and B channels.	18
3.3	An Overview of GUI	24
4.1	Visualisation of ITA classification threshold within the L* and b* color space, used for determining skin tone categories. The left side shows the skin color volume on the L*-b* plane with indicative angles for various skin tones, while the right side presents specific ITA ranges with corresponding skin tone classifications from I (very light) to VI (dark). Our dataset encompasses a diverse spectrum of skin tones, including categories from dark (Skin Type VI) to light (Skin Type II). Image taken from [2]. . .	27

4.2	Example of a baseline models. Widely available and easily reproducible baseline methods are selected for comparison. Specifically, Adobe Photoshop(PS) is chosen For <i>pixel space</i> editing methods, which is the most commonly used image editing and retouching software. For <i>latent space</i> editing methods, Stable Diffusion(SD), recognised for its high-quality generation, is selected.	29
4.3	Metadata of panellists. The test population covers people from 19 to 45 years old, multiple races, and multiple skin tones	31
4.4	Examples of questions in the questionnaire. 48 questions of such question are designed, with 24 featuring modified images. For each panellist, 10 questions are randomly selected from the question bank.	32
5.1	Simulation under various skin tones with zoomed-in details. Blue Arrows are manually added to highlight blemishes of interest (acne or pigmentation). And the skin tone classification is labeled on the side of the figure. Note that the proposed method keeps skin details (e.g., hairs, texture) unaltered and can achieve realistic blemish removal under different skin tones.	33
5.2	The application of the proposed method to the simulation of the fading process of skin blemish is shown. Blue Arrows are manually added to highlight blemishes of interest (acne or pigmentation). In the simulation, images of <i>Week 0</i> are input and the parameters of the obtained model are adjusted to simulate the change of the blemishes in the following weeks. Note that the proposed method applies to different skin tones and various types of blemishes.	34
5.3	Comparison with baseline methods on various skin tones. The results of several blemish removal or modification methods are compared, including the proposed method (marked as Proposed), Adobe Photoshop [3] inpainting (marked as PS), and Stable Diffusion [4] inpainting (marked as SD). Arrows are manually added to highlight areas of interest. Note the red arrows where the PS produces over-smoothed skin patches and the SD produces visible artifacts. For darker skin tones, the SD method fails to simulate varying intermediate states of blemish removal, displaying similar results under different control intensities.	36
5.4	Matrix of different chromophore concentrations setting. The original image is marked by a red box. The proposed model fully decouples the major chromophores of human skin, enabling highly controllable blemishes editing.	37

List of Tables

4.1	Summary of Dataset Statistics	27
5.1	FID scores of different blemish fading rates. Lower scores are better.	35
5.2	Key Statistics and Score Distribution from the Image Perception Study	38

Chapter 1

Introduction

1.1 Background

Facial appearance plays a pivotal role in an individual's self-confidence and perception of health and beauty. Among the various factors that contribute to facial aesthetics, the presence of facial blemishes such as acne and pigmentation is critical. These imperfections not only affect physical appearance but also have significant psychological and emotional consequences. Consumers across different age groups and skin tones use various skin treatments such as topical skincare products, chemical peeling, laser treatment, etc. to treat these blemishes and improve their skin appearance [5].

The relentless pursuit of beauty has catalyzed the growth of an expansive skincare market. The increasing demand for aesthetic improvement from consumers has driven skincare manufacturers to seek intuitive tools that can vividly demonstrate the long-term benefits of their products. Such a tool would enable consumers to visualize and trust the efficacy of skincare products without the need for extensive real-image data collection. Additionally, it would allow manufacturers to gather user feedback objectively, measure the therapeutic effectiveness of their products, and refine their offerings to better meet consumer needs. This pursuit aligns with a broader trend where visual representation and consumer

trust are paramount, and where the market's ability to provide clear evidence of product benefits can significantly influence purchasing decisions.

1.2 Motivation

However, consumers often have limited ability to assess the efficacy of skincare treatments designed to address blemishes before starting a treatment [5]. There is a dearth of effective models that can convey the visually appealing changes of blemish evolution to consumers, making the choice of the right skincare product to be more a trial-and-error process, during which individuals may need to use the product for a period of time to see the skin improvement. With robust blemish simulation tools, this uncertainty could be addressed. Furthermore, these tools would enable researchers and product developers to quantitatively assess how different formulations and ingredients impact the appearance of facial blemishes over time.

Although some algorithms currently focused on facial image retouching and achieving the goal of removing skin blemishes while retaining the skin texture details, they are usually designed to beautify facial images to be posted to social media [6–8]. These algorithms, adept at completely removing blemishes, lack the capability to represent the gradual and nuanced effects of blemish recovering process due to skincare treatments. This is partially due to the complex physiological and optical properties of skin, presenting a significant challenge in developing a model that accurately measures and simulates the appearance and evolution of skin blemishes.

Recent deep generative models, such as Generative Adversarial Networks [9] (GANs) and diffusion models [4, 10], have made prominent progress in image generation and manipulation, there are two main challenges in applying such

methods in the blemish simulation task. The first challenge is the collection and labelling of a large amount of high-fidelity skin data. It is well known that deep generative models are data-starving. Lacking a large amount of high-quality training data leads to unrealistic output, artifacts, or even modal collapse. The second challenge is the difficulty of defining the distributions and variations of skin blemishes. The deep generative model is intrinsically conducting distribution mapping on images. While it is easy to define distributions in the task of style transfer [11–13] according to image styles, such as art painting and sketching, the appearance status of acne and pigmentation, it improves or worsens, is hard to classify due to the lack of properly labelled data. Thus, the output of a deep neural network could have entangled features, creating an unacceptable perception to users.

1.3 Objectives and Specifications

Motivated by the above discussion, parametric techniques are sought to achieve lightweight and stable simulation and a physics-based modelling method for simulating skin acne and pigmentation changes is proposed. It is rooted in the domain knowledge of skin physiology and optics research that the appearance of facial skin blemishes: acne, and pigmentations, are related to subcutaneous melanin and haemoglobin chromophores [14]. And the unique appearance of skin blemishes is rendered by scattering properties of skin tissue [1]. First, a color space transformation is conducted to extract chromophore components from sRGB images. Based on the skin scattering properties, the relative spatial distributions for each component are then constructed by Sum-of-Gaussians. This enables the proposed method to perform realistic blemish simulation, precisely modifying the appearance of facial blemishes by tuning the parameters of the fitted model.

To validate that the proposed method can achieve realistic results, a visual comparison study was first conducted to compare simulated images and the ground-truth images from a self-collected dataset, where temporal data reflects long-term skin blemish changes. The results demonstrated that a high degree of realism is achieved by the simulations when compared to ground-truth images. Secondly, the proposed method was compared with some current generalized image editing/generation algorithms or software. Compared to these methods, the proposed method achieved natural-looking editing of skin blemishes with lower FID scores while producing fewer artifacts than deep learning methods. Furthermore, a visual perception study was conducted to quantitatively assess the discernment abilities of individuals between simulated images and authentic ones. The findings demonstrated that the approach generates realistic representations of skin blemish changes.

1.4 Major contribution of the Dissertation

This innovative approach not only addresses a pressing need in the skincare industry but also promises to impact the product development processes. By providing a reliable tool for simulating and assessing skin blemish changes, the proposed methodology equips skincare researchers and developers with the means to create more effective and targeted products. Moreover, it empowers consumers to make informed choices regarding their skincare routines. The contribution of this work is summarized as follows:

- The problem of blemish change simulation is identified, utilizing a physics-based modelling approach to approximate the physiological and optical properties of the skin. By adjusting the parameters of the fitted model, the appearance of skin blemishes can be modified, thereby achieving blemish change simulation.

- The visualization results and perception study demonstrate that the proposed method achieves a realistic skin blemish change simulation, suggesting that the physics-based modelling technique is a robust tool for skin science research.
- The research provides a new use case for the application of computer vision algorithms in the skincare and cosmetic industry, offering promising prospects in product development and serving as a powerful tool to visualize blemish changes, thus giving customers a more intuitive display of product effects and promoting sales. It also extends existing blemish retouching methods by offering a gradual and natural modification approach, which can be integrated into current face image beauty applications to enhance their realism.

1.5 Organisation of the Dissertation

This dissertation is organized as follows:

- **Chapter 2** delves into existing literature and technological advancements, providing a thorough background on skin modelling techniques. It first reviewed the definition and physiological features of skin blemishes. Then, it briefly discusses the skin optical models commonly used in realistic skin rendering, whose assumptions and simplified models form the basis for the method proposed in this thesis. Finally, it reviews current face image editing and retouching approaches to identify gaps from multiple angles: the lack of gradual and realistic evolution, the need for face blemish dataset with diverse skin tones, and the limitations in capturing the nuanced and progressive changes in skin appearance.
- **Chapter 3** presents the core methodology of the research, introducing pro-

posed novel method from the principles of skin optic and skin physiology to implementation. It starts with the Beer-Lambert law to model the relationship between chromophore concentration and image pixel values, and proposes to decompose RGB color space into chromophore color space, and then to separate the facial skin image into base and blemish layer. Then, it discusses how to use the Sum-of-Gaussian to approximate the distribution of chromophore, as well as how to modify the input image to achieve a gradual and natural manipulation of skin blemishes. Finally, it presents the algorithm optimization design, pseudocode implementation, and graphic user interface design.

- **Chapter 4** thoroughly assesses the simulation algorithm's authenticity and natural appeal through various tests, encompassing both objective and subjective reviews. This chapter details experimental design aspects like parameter choices, data collections, and methodologies. It also highlighting the dataset's comprehensiveness in terms of image resolution, diversity of skin types, and the range of blemishes represented, making it apt for testing the proposed model's efficacy.
- **Chapter 5** articulates the results and insights gained from the conducted experiments. It describes both objective and subjective tests carried out to validate the model. Objective evaluations include comparisons with existing image retouching or generation methods using objective metrics, while subjective tests involve human panel assessments to gauge the naturalness of the simulated skin changes.
- **Chapter 6** summarizes the key techniques of this method, highlighting its advantages. It also discusses its limitations and shortcomings. Finally, it explores the proposed method's application prospects and directions for improvement.

Chapter 2

Literature Review

In this chapter, the definition and physiological features of skin blemishes are first reviewed. Then, the field of computer graphics is examined, discussing how to model skin and blemishes to achieve realistic skin image rendering. Finally, attention is turned to the field of computer vision, where state-of-the-art image modeling and editing methods are reviewed, assessing the degree of fit and gaps between the goals of this task and existing methods.

2.1 Skin Chromophores & Blemishes

What gives human skin its diverse colors? When light is transmitted into the skin, energy of different wavelengths is selectively absorbed by the chromophores, scattered by the skin tissues and then observed in unique colors. The color of human skin and skin blemishes is primarily influenced by several key chromophores, namely *Melanin*, *Hemoglobin*, *Carotene*, and *Bilirubin*. These pigments, each with unique optical properties, contribute to the skin's overall coloration and appearance:

- **Hemoglobin** Found in red blood cells, Hemoglobin gives blood its red color. The optical properties of Hemoglobin vary between its two forms:

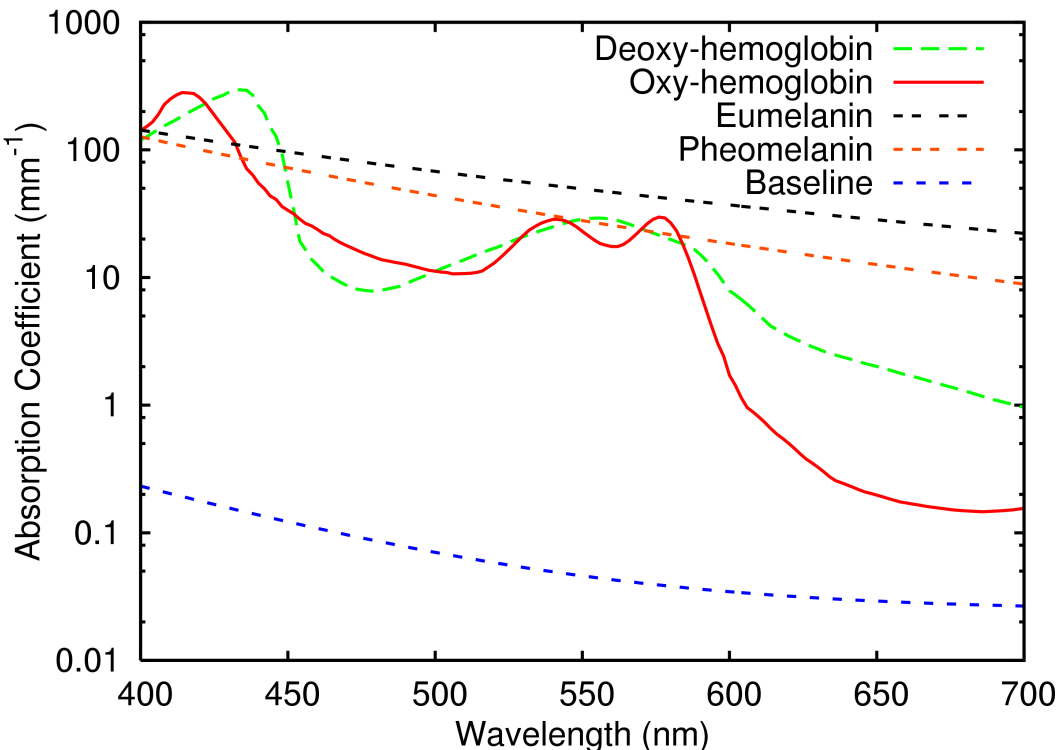


Figure 2.1: Spectral absorption coefficients of skin chromophore. This work focused on modelling heamoglobin and melanin distribution of skin blemishes. Image taken from [1]

oxy-Hemoglobin (oxygen-rich) and deoxy-Hemoglobin (oxygen-poor). These forms have distinct absorption peaks in the visible spectrum, contributing to the reddish undertones of skin.

- **Melanin** Rather than being a singular entity, Melanin is a composite of various polymers, exhibiting a spectrum of shades ranging from pale yellow to deep brown or black. The lighter variants of melanin predominantly consist of *pheomelanin*, whereas *eumelanin* typically constitutes the darker forms of melanin [15]. This is the primary determinant of skin color [16], providing shades from light to dark. Melanin absorbs across a broad range of the visible spectrum but particularly in the ultraviolet (UV) region [17]. This absorption is crucial as it protects the skin from UV radiation damage.
- **Carotene and Bilirubin** These pigments impart a yellowish hue to the

skin. They absorb light in the blue region of the spectrum, which complements the reds of Hemoglobin and the browns of melanin, contributing to the overall skin tone [17].

In this work, mainly hemoglobin and melanin in the skin are considered. For the other chromophores and their appearance, they are used as residual terms. In Figure 2.1, the spectral absorption coefficients of these two key chromophores are shown. Both types of hemoglobin have high absorption coefficients from 400nm to 450nm and from 520nm to 600nm, giving the skin a pink color appearance. Melanin, on the other hand, absorbs UV and blue-violet more strongly, giving the skin a brown to black appearance.

The formation of skin blemishes, such as pigmentations or acnes, is often associated with an overproduction or uneven distribution of skin chromophores. These blemishes can result from various factors, including genetic predisposition, hormonal changes, sun exposure, and aging. In response to UV radiation, Melanocytes (melanin-producing cells) increase their production of melanin as a protective mechanism, which can lead to localized darkening of the skin.

2.2 Skin Modeling & Rendering Techniques

Modeling skin as a layered, semi-transparent material has become common practice in studying the optical properties of skin and realistic skin rendering [1]. In this model, the interactions of light with the skin can be thought of as combinations of the following:

1. **Specular reflection:** The Figure 2.2 shows light reflecting off the surface of the skin, as indicated by the bold and yellow arrows labeled *Specular*

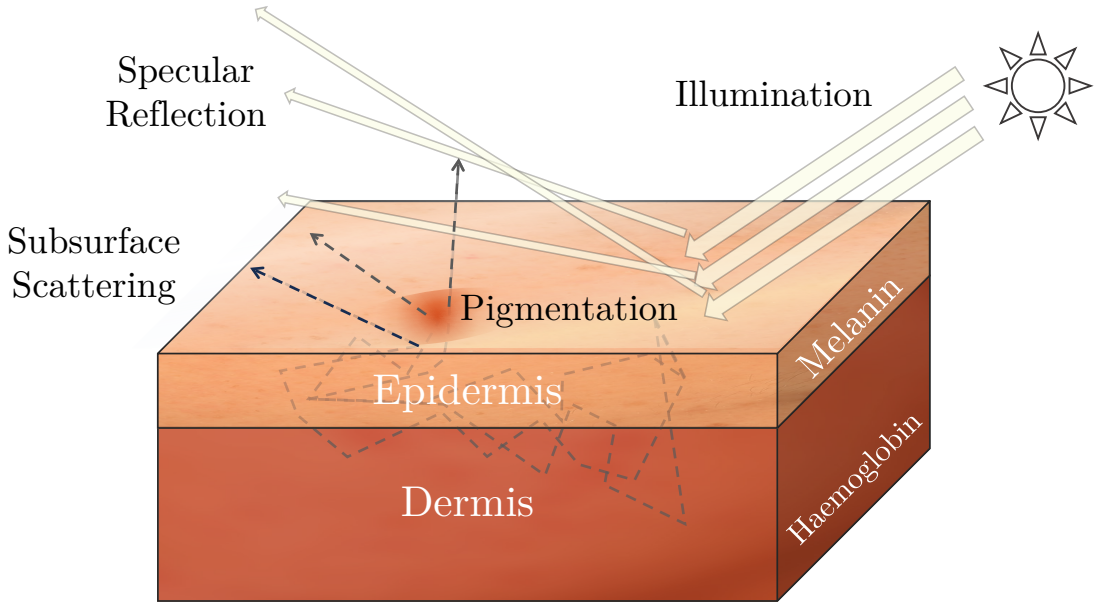


Figure 2.2: Layered skin model. A portion of the incident light undergoes specular reflection, revealed as a skin texture layer. The other part transmits into and is scattered by the Epidermis and Dermis. Melanin and haemoglobin, which are distributed in these two layers, absorb specific wavelengths of light, rendering the skin's characteristic color.

Reflection. Light reflection from the surface, caused by oils, water, and stratum corneum of the skin. It captures the surface texture of the skin, such as fine grooves and textures. The proposed method preserves these details unaltered.

2. **Subsurface scattering and absorption:** Physiologically, skin is semi-transparent [18]. Skin constituents such as extra-cellular matrix cause random deflections of incoming light rays, some of which are reflected back to the surface and are observed. This phenomenon is called subsurface scattering. The Figure 2.2 illustrates how light penetrates the skin layers and scatters within, a process depicted by the dashed lines under the surface. In addition, as shown in Figure 2.2, the chromophore components present in the epidermis and dermis layers, such as melanin and haemoglobin, selectively absorb light propagating in the skin, thus rendering the unique hue of human skin. When chromophore is locally accumulated, it will render a blemish where the color is different from the surrounding skin [17]. The

proposed method emphasizes this unique optical phenomenon to achieve realistic blemishes modelling and editing.

3. **Transmission:** When the light is very strong and shines on thin tissue (such as the ears or fingers under strong light), a unique transmission appearance can be observed against the light source. For blemish change modelling, this aspect is disregarded and do not draw in Figure 2.2.

Despite the multilayer skin model describing the unique appearance resulting from skin optical properties well and conforming to the physiological structure of real skin, rendering realistic skin images on a computer has been challenging.

Thanks to advancements in modern graphics hardware and developments in computer graphics, realistic skin rendering can now be achieved [19–21]. The key lies in achieving an accurate and efficient simulation of the subsurface scattering behavior of the skin. Although ray tracing and path tracing [22, 23] are regarded as some of the most realistic approximations for the behaviors of light rays, these methods often require massive computations and can be difficult to apply to real-time scenarios, so approximate fast algorithms become the primary consideration. Jensen et al. [24] proposed the Bidirectional Surface Scattering Reflectance Distribution Function (BSSRDF) to approximate the light transmission function. Based on their observations and assumptions, in highly scattering media, light scattering tends to be isotropic, so the scattering distribution is only related to the distance from the incident point. Based on this assumption, Eugene et al. [25] proposed using a diffusion profile to describe this scattering distribution, thereby achieving efficient and realistic skin rendering. However, it is still challenging to accurately simulate the scattering of the multilayer skin model. Fortunately, Jensen et al. [26] pointed out that using the sum of 4 or more Gaussian functions to approximate the diffusion profile of the multi-layer skin model has been proven to be very effective in practice. Moreover, they

calculated a set of well-fitted parameters and successfully simulated the diffusion distribution of the multi-layer skin model in the RGB domain.

These methods have inspired the work to take into account the optical properties of the skin in the proposed algorithm, thus achieving realistic blemish simulation.

2.3 Controllable Facial Image Editing

2.3.1 Objectives and Definitions

Deep learning-based methods, notably Generative Adversarial Networks (GANs) and Diffusion models, have been instrumental in image content editing, learning a projection from latent noise to pixels [9, 10, 27]. Control over the generated image in these methods is typically achieved through latent space manipulation [28, 29]. After training, additional precise control over these methods requires embedding control parameters within the input noise or the model's pipeline, often using techniques like Low-Rank Adaption (LoRA) [30] or ControlNet [31]. However, these methods necessitate extensive data annotation and model fine-tuning for effective and accurate editing.

Contrastingly, this research adopts a physics-based modelling approach, which focuses on the optical and physiological properties of skin. By employing a Sum-of-Gaussians fitting, it facilitates control over the shape, color, and size of local skin blemishes. This approach simulates their natural degradation process, functioning effectively without extensive training datasets, thus offering an interpretability advantage over deep learning models.

2.3.2 Dataset and Stability

The efficacy of deep learning-based methods is heavily contingent on dataset quality. These models often suffer from overfitting on small datasets, leading to repetitive generation patterns or erroneous feature associations (e.g., linking specific skin tones to gender or age). Moreover, the absence of samples depicting gradual changes in the same subject hampers the model’s ability to learn realistic trajectories.

Although recent advancements in high-resolution portrait datasets [28] have propelled deep learning models in face image generation, these datasets primarily encompass coarse features like face shape and expression. Skin texture datasets, such as those proposed in Bai et al. [32], offer insights into skin rendering. However, they typically showcase near-perfect skin textures, lacking in representations of skin anomalies or diseases. Recent works have been explored for skin pigmentation generation [33] but lack explicit control over the output nor the ability to modify existing images.

In contrast, the proposed method introduces a novel physical-based model that operates independently of paired image datasets. This approach circumvents the limitations imposed by the lack of comprehensive and diverse data typical in deep learning frameworks. By modeling the optical and physiological characteristics of skin using a Sum-of-Gaussians approach, it enables the simulation of natural blemish fading processes with high fidelity. The independence from paired image datasets not only reduces the reliance on extensive data collection and annotation but also enhances the model’s applicability to a broader range of scenarios and skin types, making it a significant advancement in the field of facial image editing.

2.3.3 Controllability

In this section, the categorization of image content editing methods into three distinct classes is presented: Pixel Space, Latent Space, and Parameter Space.

- **Pixel Space:** This class includes methods operating at the pixel level, such as inpainting and filtering. Inpainting techniques use neighboring or similar pixels for blemish correction [34–36]. However, these approaches often result in unnatural editing due to simplistic interpolation and blemish pixel detection via hard thresholding. Filtering methods apply content-aware smoothing to maintain skin details while removing blemishes [37, 38], but they do not fully address the gradual fading of blemishes.
- **Latent Space:** Deep generative models, such as those proposed by Goodfellow et al. and Rombach et al., map latent noise to pixels [4, 9]. This approach, termed latent space editing, has been applied in skin pigmentation generation and face image retouching [6, 33, 39]. While these models facilitate smooth image transitions, they often lack explicit control for modifying existing images.
- **Parameter Space:** Referred to as Parametric Space editing, this category involves physics-based methods that model skin optics and physiology. By adjusting model parameters, facial image modification is achieved [14, 40]. Lin et al. introduced a method for modifying chromophore content in pigmentation, focusing on holistic adjustments [7].

The proposed method introduces an innovative physical-based model enabling precise, per-blemish chromophore concentration modeling and retouching without relying on paired image datasets. This approach, utilizing logarithmic RGB space decomposition, more accurately represents chromophore light absorption. It accounts for blurred blemish edges due to subsurface scattering, enabling

seamless integration with the surrounding skin. This method stands out for its unprecedented control over blemish modifications attributed to localized chromophore accumulation, marking a novel advancement in this field.

Chapter 3

Methods

3.1 Skin Chromophore Color Space Decomposition

In digital photos, skin color represents only a small subset of the sRGB space, due to unique chromophores contained in the skin, such as melanin and haemoglobin, which give the skin a unique and limited color range. However, finding a transformation from sRGB values to the absolute concentration of skin chromophores is challenging, as the sRGB color space is device-agnostic. It also requires calibrating the camera system using pigmentation data *in vivo*. This issue is bypassed by modeling the *relative* pigment concentration against the base skin, so that the transformed color space can well express the influence of different chromophores on skin color without the need for camera system calibration.

Specifically, the relative absorption of incident light by the chromophore can be described by the Beer-Lambert law, namely:

$$A(\lambda) = -\log(R(\lambda)) = C\varepsilon l, \quad (3.1)$$

where A represents absorption, R is the reflection intensity, λ is the wavelengths, C is the relative concentration, ε denotes the extinction coefficient of chromophore and l is the mean optical path length.

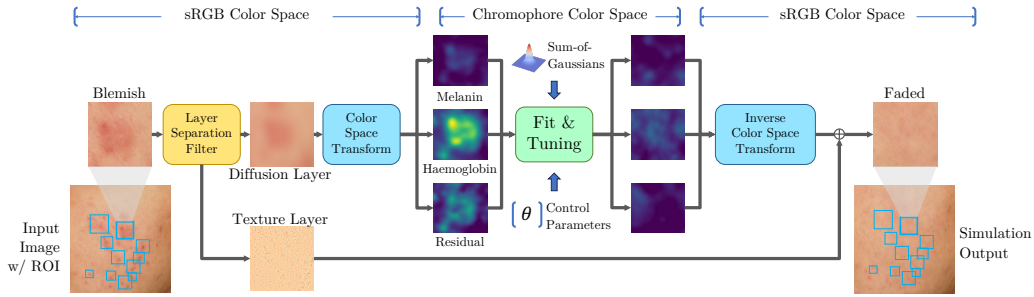


Figure 3.1: An overview of the proposed skin blemish change simulation pipeline. In the pipeline, a box of Region of Interest (ROI) is first used to select the blemish like acne or pigmentation. Then, a *Layer Separation Filter* is applied to separate the texture layer and the diffusion layers. A *Sum-of-Gaussians* model is fitted to each ROI in *Melanin/Heamoglobin* color space, with the parameters of the fitted model adjusted to manipulate the appearance of the blemishes. The modified diffusion layer is summed with the original texture layer to obtain the output.

In this work, the impact of two chromophores on the skin, melanin and heamoglobin, and a residual term, are mainly considered, as shown in Figure 2.2. Therefore, $C\epsilon l$ in equation 3.1 expands as

$$A(\lambda) = C_H \epsilon_H(\lambda) l_H + C_M \epsilon_M(\lambda) l_M + C_r \epsilon_r(\lambda) l_r, \quad (3.2)$$

where subscript H , M , and r represent heamoglobin, melanin, and residual chromophore, respectively.

Given the distinct absorption and reflection properties of skin chromophores under varying wavelengths of light, the response of each chromophore is considered across the three primary camera pixel channels: Red (\mathcal{R}), Green (\mathcal{G}), and Blue (\mathcal{B}). This consideration leads to the formulation of Equations 3.1 and 3.2. These equations model the chromophore response in the context of the color channels, providing a foundation for further analysis and image processing within the scope of the proposed method.

$$C_H \epsilon_H^c l_H + C_M \epsilon_M^c l_M + C_r \epsilon_r^c l_r = -\log(R^c) \quad (3.3)$$

$$c \in \{\mathcal{R}, \mathcal{G}, \mathcal{B}\},$$

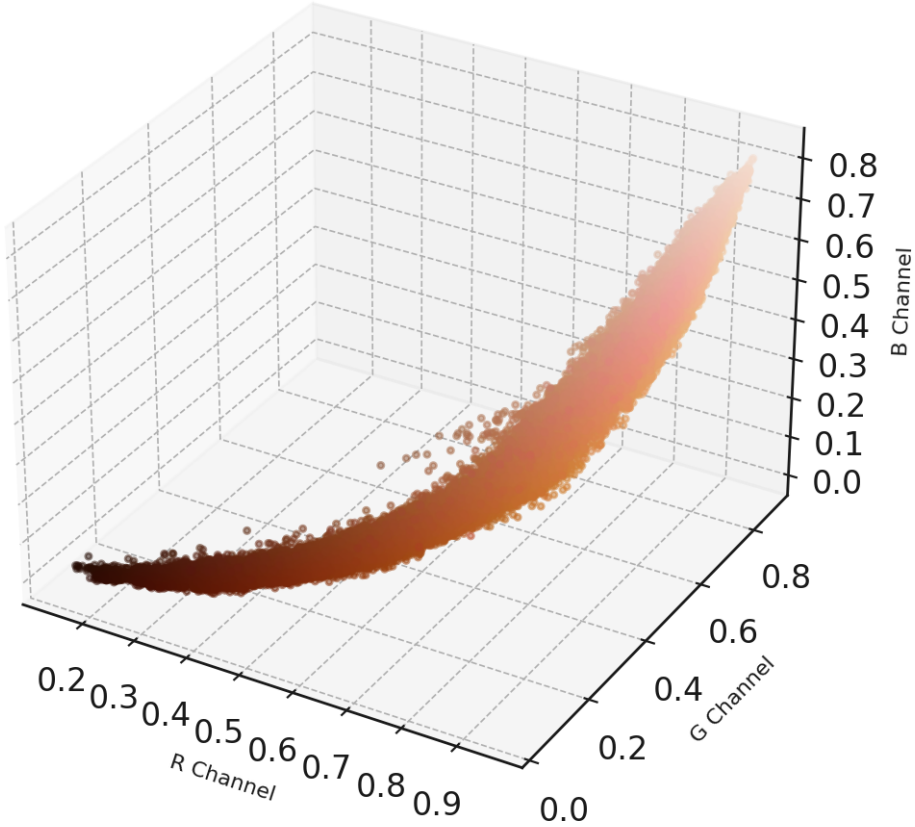


Figure 3.2: 3D scatter plot showing the distribution of skin colors sampled from the face skin images in a dataset, illustrating the correlation between the R, G, and B channels.

or in matrix form

$$\mathbf{E}\mathbf{c} = -\log(\mathbf{k}),$$

$$\mathbf{E} = \begin{bmatrix} \varepsilon_H^{\mathcal{R}} l_H & \varepsilon_M^{\mathcal{R}} l_M & \varepsilon_r^{\mathcal{R}} l_r \\ \varepsilon_H^{\mathcal{G}} l_H & \varepsilon_M^{\mathcal{G}} l_M & \varepsilon_r^{\mathcal{G}} l_r \\ \varepsilon_H^{\mathcal{B}} l_H & \varepsilon_M^{\mathcal{B}} l_M & \varepsilon_r^{\mathcal{B}} l_r \end{bmatrix}, \quad \mathbf{c} = \begin{bmatrix} C_H \\ C_M \\ C_r \end{bmatrix}, \quad \mathbf{k} = \begin{bmatrix} R^{\mathcal{R}} \\ R^{\mathcal{G}} \\ R^{\mathcal{B}} \end{bmatrix}.$$

It is reported that there is no significant difference in skin thickness between human races [41]. In other words, l can be seen as a constant. So l is combined with ε in \mathbf{E} . Following the practice of Tsumura et al. [42], E is estimated by Fast Independent Component Analysis (FastICA) [43] in the log-RGB domain. Specifically, 128 patches are randomly sampled from each face skin image of the dataset, and each patch is 16x16 pixels in size. Then the av-

verage RGB value of each patch is calculated, as illustrated in Figure 3.2. The FastICA algorithm in `sklearn` [44] is adopted to estimate the 3 independent components over the log-RGB domain as \mathbf{E} . In this work, $\hat{\mathbf{E}}$ is obtained as follows:

$$\hat{\mathbf{E}} = \begin{bmatrix} 0.96 & -0.63 & 0.9 \\ -0.22 & 0.35 & 0.17 \\ -0.16 & -0.69 & -0.4 \end{bmatrix} \quad (3.4)$$

3.2 Blemishes Appearance Modelling & Editing

Given a 3-channel image patch $C(\mathbf{x}) \in \mathbb{R}^{3 \times h \times w}, \mathbf{x} \in \mathbb{R}^2$ with length w and height h , containing a user-selected blemish, it assumes that the patch can be divided into normal skin C_K^{skin} and blemish C_K^{blem} in chromophore color space, that is

$$C_K(\mathbf{x}) = C_K^{skin}(\mathbf{x}) + C_K^{blem}(\mathbf{x}), \quad K \in \{H, M, r\}. \quad (3.5)$$

For the estimation of C_K^{skin} , it assumes that skin color changes are smooth within a local area. Therefore, it can be fitted by a simple linear model

$$\hat{C}_K^{skin}(\mathbf{x}; \mathbf{k}, d) = \mathbf{k}\mathbf{x} + d, \quad \mathbf{k} \in \mathbb{R}^2, d \in \mathbb{R}. \quad (3.6)$$

For the estimation of C_K^{blem} , the proposed method is based on the observation that pigmentation and acne of interest tend to have blurred edges due to the subsurface scattering of light under the skin. On one hand, they are caused by local accumulation of chromophores under the skin due to various stressors such as UV or inflammation, which can be modeled as Gaussian distributions. On the other hand, subsurface scattering of light under the skin makes blemishes look even blurry. With Gaussian functions, both phenomena can be described very well, because the convolution of two Gaussian functions is still a Gaussian

function, namely:

$$\begin{aligned} G(x; \mu_a, \sigma_a, a) * G(x; \mu_b, \sigma_b, b) \\ = a \cdot b \cdot G(x; \mu_a + \mu_b, \sqrt{\sigma_a^2 + \sigma_b^2}), \end{aligned} \quad (3.7)$$

where $*$ is the convolution operator, and Gaussian function G is defined as

$$G(x; \mu, \sigma, a) = \frac{a}{\sigma \sqrt{2\pi}} e^{-\frac{(x-\mu)^2}{2\sigma^2}}. \quad (3.8)$$

For multivariate Gaussian functions (2D in this research), they can be denoted as

$$G(\mathbf{x}; a, \mu, \Sigma) = \frac{a}{2\pi \sqrt{|\Sigma|}} e^{-\frac{1}{2}(\mathbf{x}-\mu)^T \Sigma^{-1} (\mathbf{x}-\mu)}, \quad (3.9)$$

where $\mu = [\mu_x, \mu_y]^T$ is the centre coordinate (x, y) on the input image plane, $\Sigma \in \mathbb{R}^{2 \times 2}$ is the covariance matrix and a is the amplitude factor. And note that the above conclusion can also be generalized to this multivariate case.

To better fit variously shaped blemishes and uneven facial areas, Σ can be further decomposed into multiplication of rotation matrix \mathbf{R} and scaling matrix \mathbf{S} as

$$\Sigma = \mathbf{R} \mathbf{S} \mathbf{R}^T. \quad (3.10)$$

This allows Gaussian functions to stretch and off-axis rotation with an angle of $\theta \in [0, \pi)$, forming ellipsoidal patterns, that is

$$\mathbf{R} = \begin{bmatrix} \cos \theta & -\sin \theta \\ \sin \theta & \cos \theta \end{bmatrix}, \quad \mathbf{S} = \text{diag}(\sigma_x, \sigma_y). \quad (3.11)$$

Or explicitly

$$\begin{aligned} G(x, y; \mu_x, \mu_y, \sigma_x, \sigma_y, \theta, a) \\ = \frac{a}{2\pi \sigma_x \sigma_y} \cdot e^{-\frac{x''^2}{2\sigma_x^2} - \frac{y''^2}{2\sigma_y^2}}, \quad \text{where} \end{aligned} \quad (3.12)$$

$$x' = x - \mu_x, \quad y' = y - \mu_y,$$

$$x'' = x' \cos \theta - y' \sin \theta, \quad y'' = x' \sin \theta + y' \cos \theta.$$

Finally, following the existing fast subsurface scattering implementations, the ap-

pearance of a blemish under the scattering skin tissue is approximated by sum of multiple Gaussian functions. That is, the estimated distribution $C_K^{\hat{b}lem}(\mathbf{x})$ can be denoted by

$$C_K^{\hat{b}lem}(\mathbf{x}; \Theta) = \sum_{i=0}^{N-1} G_i(\mathbf{x}; \Theta_i), \quad N \geq 1, \Theta_i = [a_i, \mathbf{S}_i, \mu_i, \theta_i]. \quad (3.13)$$

The parameters are fitted by the Levenberg-Marquardt method [45] with the lmfit Python library [46]. After successful fitting, $C_K^{\hat{skin}}$ is discarded. Instead, $C_K^{\hat{b}lem}$ is multiplied with a user-input gain $\alpha_K \in \mathbb{R}$ and add it with the input $C_K(\mathbf{x})$ to amplify/attenuate the blemish intensity to obtain the modified image patch C'_K , namely

$$C'_K = C_K + \alpha_K C_K^{\hat{b}lem}. \quad (3.14)$$

Obviously, if $\alpha_K = -1$, the facial blemish will be completely removed from the image patch, while a positive gain will intensify this blemish.

3.2.1 Algorithm Implementations

Preporcessing

In the proposed methodology, as depicted in Figure 3.1, the primary focus is laid on the *Diffusion Layer* of the image. To isolate this layer, a skin layer separation filter is first adopted to separate the skin into a surface *Texture Layer* (including specular reflections and skin textures) and a *Diffusion Layer*. This is implemented using a Gaussian filter with a small variance, small enough to isolate the detail texture of the skin without affecting the underlying assumptions.

Subsequently, in color space transform stage, inverse gamma correction is applied to the standard RGB (sRGB) image to derive linear RGB values. These values are then converted to their logarithmic form, representing an approxima-

tion of the real reflectance values, denoted as R in Equation 3.1. While this approximation may not perfectly mirror the actual scenario, it proves adequate for estimating the relative concentration ratio in comparison to the surrounding skin.

Optimizations in Fitting Process

In the actual implementation, several optimizations are performed to the program:

- Each channel and each blemish can be fitted independently and multi-process parallelism can be used to speed this up. Thus, the program packages each fitting session into a task and uses Python’s thread pool to build a task queue, fully utilizing the computing power of multi-core CPUs.
- Although the entire Sum-of-Gaussians model could be fitted at once, the convergence of the fit would be slow. Therefore, a strategy is adopted where a new N -th Gaussian function is gradually introduced into the model with $N-1$ functions and the updated model is fitted, during which the existing parameters are frozen. Finally, all parameters are unfrozen for one more fitting as a fine-tuning. In this way, only one function is fitted each time except for the last one.
- In Levenberg-Marquardt iterations, it requires compute the Jacobian matrix for each steps. Since each component in \hat{C}_k has explicit partial derivatives and they are just simply summed together, the Jacobian matrix of \hat{C}_k can be manually derived. This assists the Levenberg-Marquardt algorithm to quickly compute accurate gradients rather than estimate them numerically.

This algorithm can be represented by the following pseudocode.

Algorithm 1 Fitting Distribution of a Blemish

```

1: Input: Blemish image patch  $X \in \mathbb{R}^{3 \times h \times w}$ , per-channel gain  $\alpha_k \in \mathbb{R}^3$ . All
   from user-input.
2: Preprocessing:
3:  $X_d, X_t \leftarrow GaussianFilter(X)$             $\triangleright X_d$ :Diffusion Layer,  $X_t$ :Texture Layer
4:  $X_d \leftarrow \gamma^{-1}(X_d/255.0)$      $\triangleright$  Inverse gamma transformation to linear RGB space
5:  $X_d \leftarrow \mathbf{E}^{-1} \cdot \log X_d$            $\triangleright$  Transform to chromophore color space
6: for each channel  $k \in \{H, M, r\}$  of  $X_d$  do
7:   Initialize linear normal skin model  $\hat{C}_k \leftarrow C_k^{skin}$ 
8:   for each Gaussian component  $G_k^i$  do
9:     Fit  $G_k^i(x, y; \mu_x^i, \mu_y^i, \sigma_x^i, \sigma_y^i, \theta^i, a^i)$ 
10:     $\hat{C}_k \leftarrow \hat{C}_k + G_k^i$ 
11:    Freeze parameters of  $\hat{C}_k$ 
12:  end for
13:  Unfreeze all parameters for final refinement fit
14:   $\hat{C}_k \leftarrow \alpha_k \cdot (\hat{C}_k - C_k^{skin})$ 
15: end for
16:  $X_d \leftarrow X_d + \hat{C}_k$ 
17:  $X_d \leftarrow InverseColorTransform(X_d)$ 
18:  $X \leftarrow X_d + X_t$ 
19: Return: Fitted parameters and modified blemish image

```

GUI Implementations

As shown in Figure 3.3, a simple graphical user interface (GUI) is also created to facilitate the editing of facial images by users with varying levels of expertise. The GUI is organized into several sections, each providing tools for specific tasks in the editing process.

- **Image Upload and Blemish Selection** The initial interaction with the interface is the image upload functionality, denoted by circled numeral 1 in Figure 3.3. Users can upload the facial image they intend to edit. Following the upload, the image is displayed within the central work area of the GUI, allowing users to identify and select skin blemishes for removal or modification. This selection process is designed to be intuitive, employing a simple point-and-click mechanism to mark areas of interest, as indicated by circled numeral 2.



Figure 3.3: An Overview of GUI

- **Basic and Advanced Editing Controls** After blemish selection, users can adjust the editing intensity using the 'alpha' parameter, a slider control located in the section marked by circled numeral 3 in Figure 3.3. This

allows for the manipulation of the editing gain in a user-friendly manner. Activating the 'Run' button initiates the rendering process, culminating in the display of the modified image where the selected blemishes have been processed according to the specified parameters.

For users requiring more sophisticated control, the interface offers advanced editing options as shown in circled numeral 4. This advanced control panel permits individual adjustments to the gains of separate color channels, thus affording an enhanced level of precision in the blemish editing process.

- **Parameter Exportation for Analysis** An essential feature of the GUI, highlighted in circled numeral 5 in Figure 3.3, is the ability to download the fitting results. This function caters to expert users who wish to perform a detailed analysis of the editing parameters or to utilize these parameters for further processing steps, thereby extending the capabilities of the system.

Chapter 4

Experiments

4.1 Dataset

To the best of the authors' knowledge, there is currently no dataset for studies of skin blemish modification and fading. Therefore, a self-collected dataset is adopted for research, development, and testing. The images within the dataset were acquired by two clinical imaging systems (Visia CR4 and OLE, both developed by Canfield Scientific). They were cross-polarized and color-calibrated and had a minimum resolution of 3700×5600 . The dataset consists of 223 subjects within the age range of 18 to 45 years, encompassing multi-ethnic consumers with skin tones ranging from dark to light, quantitatively assessed using the Individual Typology Angle (ITA), visualized in Figure 4.1. The ITA for each subject is calculated using the formula:

$$\text{ITA} = \arctan\left(\frac{L^* - 50}{b^*}\right) \times \frac{180}{\pi}, \quad (4.1)$$

where L^* and b^* are coordinates from the CIE-LAB color space representing the lightness and the chromaticity on the yellow/blue axis, respectively. This measure provides a valuable tool for analyzing skin tone diversity in the dataset. The collection period lasted for a duration of up to 3 months during the Summer season with a time step of one week. The summary of the dataset is

Table 4.1: Summary of Dataset Statistics

ITA Score		Ethnicity		Skin Tone Classification	
Total Subjects	223	African	126	Dark	76
ITA Mean	2.58	Caucasian	98	Brown	132
ITA Variance	851.90	Indian	108	Tan	152
		Latino	114	Intermediate	62
				Light	8

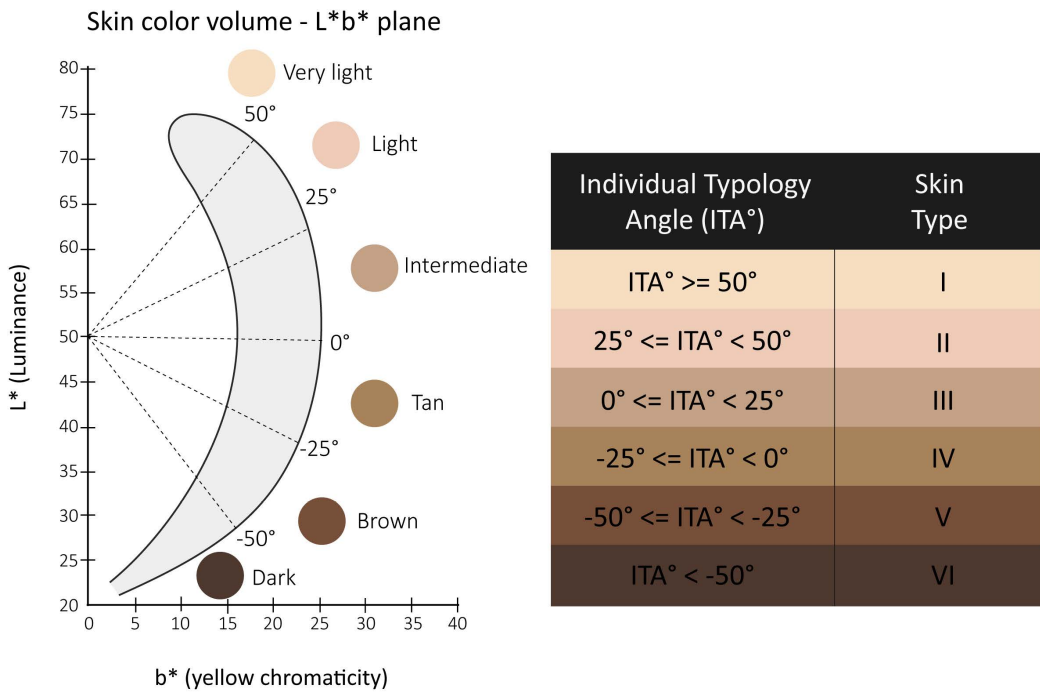


Figure 4.1: Visualisation of ITA classification threshold within the L* and b* color space, used for determining skin tone categories. The left side shows the skin color volume on the L*-b* plane with indicative angles for various skin tones, while the right side presents specific ITA ranges with corresponding skin tone classifications from I (very light) to VI (dark). Our dataset encompasses a diverse spectrum of skin tones, including categories from dark (Skin Type VI) to light (Skin Type II). Image taken from [2].

shown in Table 4.1. In the simulation, images of Week 0 are input and the parameters of the obtained model are adjusted to simulate the change of the blemishes in the following weeks. As shown in Figure 5.2, the input is labelled as *Week 0* and the images for the next few weeks as *+n W*.

4.2 Experiment Setup

In this study, extensive blemish change simulation experiments are carried out to evaluate the proposed algorithm's effectiveness. Each blemishes is fitted with 3 Gaussian functions summation and $\sigma = 10$ is set for the skin texture layer separation filter. The focus is mainly on the relative concentration changes of the blemishes, and a series of simulations are conducted based on tuning the concentration parameter after successfully fitting blemishes.

Inpainting mode of **Stable Diffusion**(SD) [4] and **Adobe Photoshop**(PS)'s inpainting tool [3] are selected for comparison as baseline models, as shown in Figure 4.2. The former, a top-performing deep learning model, represents the "latent space editing" method discussed. For the SD method, the inpainting mode is used and the text prompt is set as skin patch, human face skin, high definition, best quality, as shown in Figure 4.2a. Each test is performed with 50 iterations of sampling using the DPM++SDE Karras sampler, with the random seed fixed to 42. The denoising ratio is adjusted to increase the difference between the generated image and the original so that the intensity of blemish removal is controlled.

For the PS method, a common image editing software, represents the "pixel space editing" method. Here, the inpainting tool is utilized, selecting and removing blemishes on the original image with *Content-Aware* mode, as shown in Figure 4.2b. The modified image is then combined with the original image through Alpha blending. And the degree of blemish removal is adjusted by altering blending opacity.

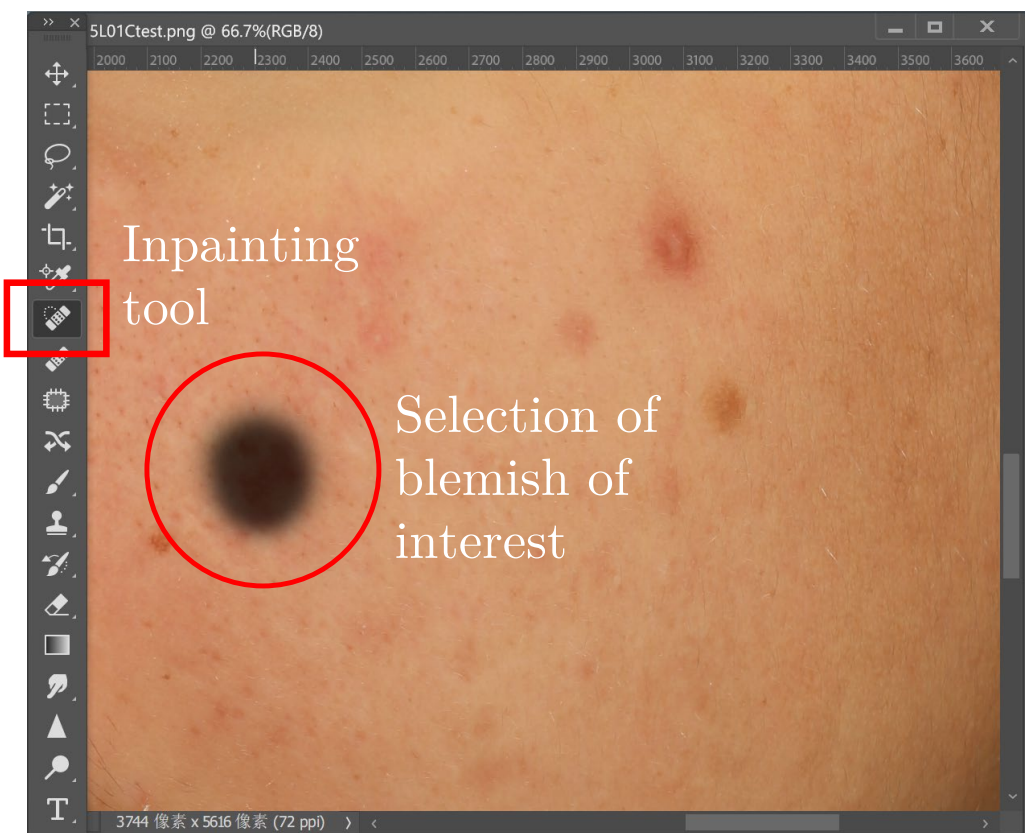
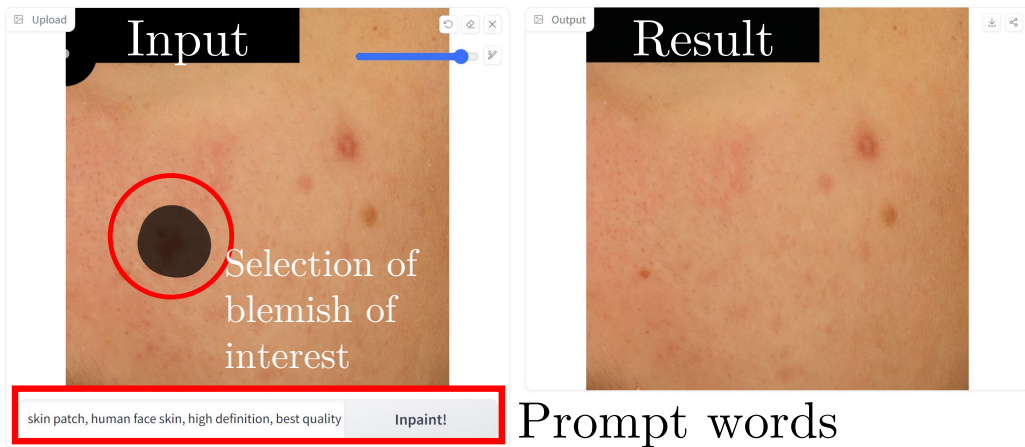


Figure 4.2: Example of a baseline models. Widely available and easily reproducible baseline methods are selected for comparison. Specifically, Adobe Photoshop(PS) is chosen For *pixel space* editing methods, which is the most commonly used image editing and retouching software. For *latent space* editing methods, Stable Diffusion(SD), recognised for its high-quality generation, is selected.

4.2.1 Objective Evaluation

To objectively evaluate image modifications, the Fréchet Inception Distance (FID) is applied. FID is a common tool for assessing GANs and similar image-generating models. It uses the Inception V3 [47] model to derive the mean and covariance matrix of feature vectors from both authentic and generated image collections. Then, it calculates the Fréchet distance between these statistical groups. This distance gauges the variation between two multi-dimensional Gaussian distributions. Generated images resembling real images more closely have lower FID scores, while higher scores show a bigger divergence. Formally, the FID score is denoted as:

$$\text{FID} = \|\mu_r - \mu_g\|^2 + \text{Tr}(\Sigma_r + \Sigma_g - 2(\Sigma_r \Sigma_g)^{1/2}), \quad (4.2)$$

where μ_r, μ_g represent the mean feature vectors of the real and generated/modified images, respectively. Σ_r, Σ_g are the covariance matrices of the real and generated/modified images, respectively. And $\text{Tr}(\cdot)$ is the trace of a matrix, which is the sum of the diagonal elements.

4.2.2 Subjective Evaluation

To subjectively evaluate the performance of the proposed facial skin blemish simulation algorithm, a visual perception study is conducted. The aim is to comprehensively evaluate whether the proposed algorithm could produce authentic and believable blemish changes and to analyse whether there are biases in certain attributes of the skin, such as skin color or age. A group of 500 panelists join this study, whose age groups are divided into three categories: 19-25; 26-34; and 35-45, covering various ethnicities including Caucasians, African-Americans, Asians, Hispanics, and others, as shown in Figure 4.3. In the survey, the question asked is *you will see a series of patches from face images*.

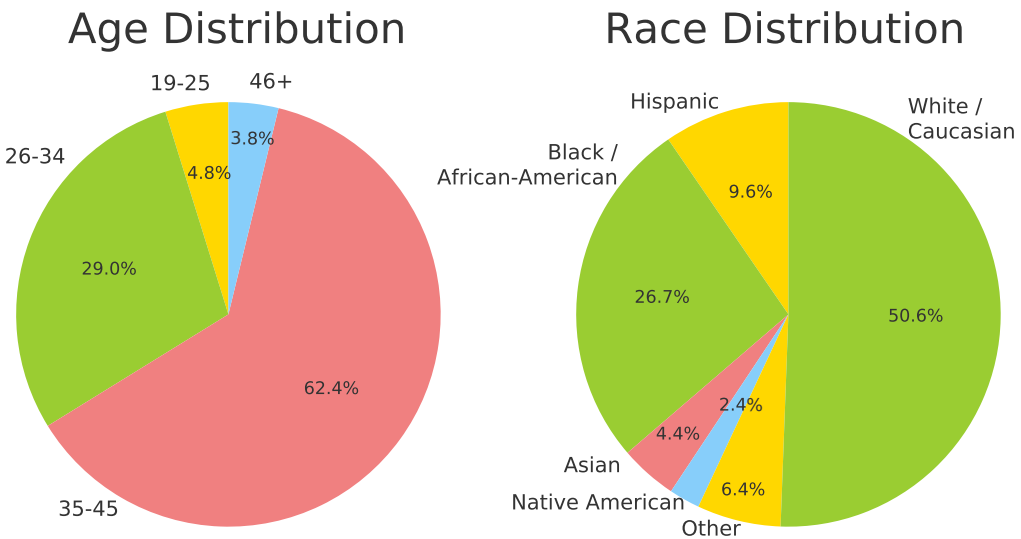


Figure 4.3: Metadata of panellists. The test population covers people from 19 to 45 years old, multiple races, and multiple skin tones

Some images have been modified so that some spots (acnes or pigmentations) on the skin have been reduced/removed by computer software. You are invited to assess how confident you are that the image you see have been modified. The answer options are set as:

- Confident that some spots on the skin image are modified/reduced (looks very unrealistic, observe significant unnatural traces of modification). (-2)
- Somewhat Confident that some spots on the skin image are modified/reduced (looks unrealistic, observe slight unnatural traces of modification). (-1)
- Not sure if any spots on the skin image are modified/reduced. (0)
- Somewhat confident that NO spots are modified/reduced (looks realistic, hardly any unnatural trace of modification). (+1)
- Confident that NO spots are modified/reduced (looks very realistic, no unnatural trace of modification at all). (+2)

In the survey, 48 images (24 simulated through the proposed algorithm and 24 unaltered images) are shown to the panellists one image at a time. When the

Section 1


In this section you will see a series of patches from face images. **Some images** have been modified so that some spots (acnes or pigmentations) on the skin have been **reduced/removed** by computer software.

You are invited to assess **how confident you are that the image you see have been modified**.

Score description:

1. **Confident** that some spots on the skin image are **modified/reduced** (looks very unrealistic, observe significant unnatural traces of modification).
2. **Somewhat Confident** that some spots on the skin image are **modified/reduced** (looks unrealistic, observe slight unnatural traces of modification).
3. **Not sure** if any spots on the skin image are modified/reduced.
4. **Somewhat confident** that **NO spots are modified/reduced** (looks realistic, hardly any unnatural trace of modification).
5. **Confident** that **NO spots are modified/reduced** (looks very realistic, no unnatural trace of modification at all).

5
1065R


Score description:

1. **Confident** that some spots on the skin image are modified/reduced (looks very unrealistic, observe significant unnatural traces of modification).
2. **Somewhat Confident** that some spots on the skin image are modified/reduced (looks unrealistic, observe slight unnatural traces of modification).
3. **Not sure** if any spots on the skin image are modified/reduced .
4. **Somewhat confident** that NO spots are modified/reduced (looks realistic, hardly any unnatural trace of modification).
5. **Confident** that NO spots are modified/reduced (looks very realistic, no unnatural trace of modification at all).

* 

1
2
3
4
5

Figure 4.4: Examples of questions in the questionnaire. 48 questions of such question are designed, with 24 featuring modified images. For each panellist, 10 questions are randomly selected from the question bank.

score ranges from 0 to +2, the respondents are considered to be affirming the image as "real" rather than modified. A sample question in the survey is shown as Figure 4.4.

Chapter 5

Result & Discussion

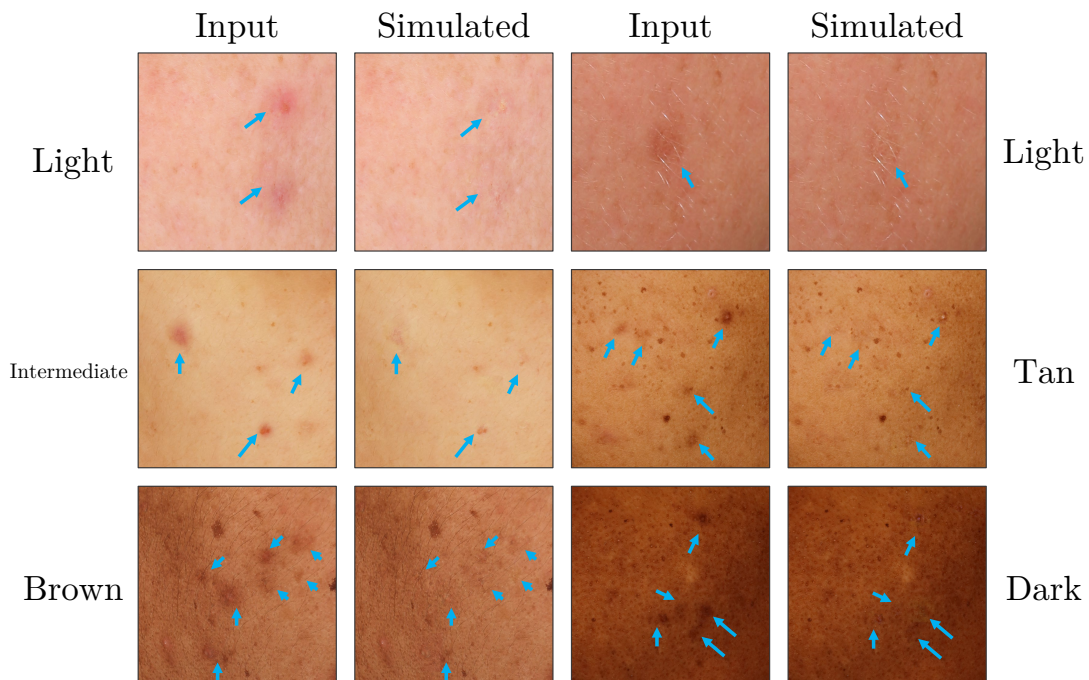


Figure 5.1: Simulation under various skin tones with zoomed-in details. Blue Arrows are manually added to highlight blemishes of interest (acne or pigmentation). And the skin tone classification is labeled on the side of the figure. Note that the proposed method keeps skin details (e.g., hairs, texture) unaltered and can achieve realistic blemish removal under different skin tones.

The simulation quality and result are evaluated in terms of versatility, reality, and controllability. A detailed discussion of each aspect follows.

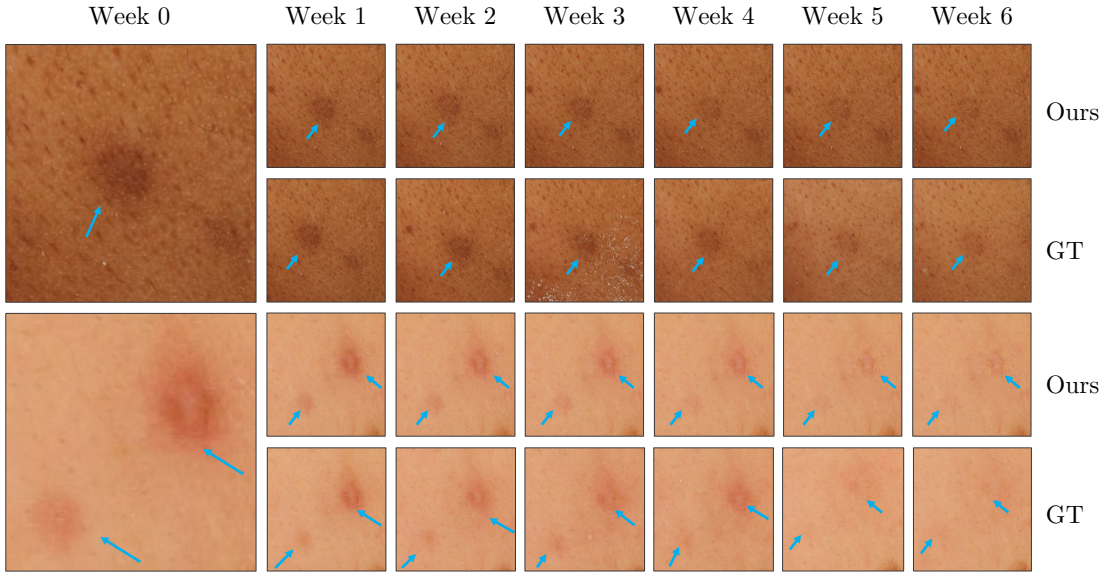


Figure 5.2: The application of the proposed method to the simulation of the fading process of skin blemish is shown. Blue Arrows are manually added to highlight blemishes of interest (acne or pigmentation). In the simulation, images of Week 0 are input and the parameters of the obtained model are adjusted to simulate the change of the blemishes in the following weeks. Note that the proposed method applies to different skin tones and various types of blemishes.

5.1 Versatility

Versatility is a key attribute of the proposed algorithm's ability to be generalized to various scenarios. By testing various patterns and degrees of pigmentation, acne, and other skin blemishes, the successful application of the proposed algorithm on multiple skin tones and different types of skin blemishes is demonstrated. Figure 5.1 clearly illustrates how the proposed algorithm accurately models the local chromophore enrichment of the skin, thus realizing genuine blemish change simulation. Particularly noteworthy is that the proposed method maintains the subtle textures of the skin unaltered, as fine hairs or pores shown in Figure 5.1, further proving its high precision and usability.

Table 5.1: FID scores of different blemish fading rates. Lower scores are better.

Methods	Fading Rate				
	100%	80%	60%	40%	20%
SD	144.89	133.53	134.16	160.10	159.54
PS	117.98	120.37	125.15	129.26	129.96
Proposed	115.30	118.12	122.64	127.09	131.60

5.2 Reality

Exploration of reality evaluates the proposed algorithm’s ability to simulate complex changes in real human skin conditions. Some skin blemish samples with long-term evolution patterns from the dataset are selected and simulated using the proposed algorithm. Figure 5.2 shows one example, revealing the gradual fading of blemishes over 7 weeks. The proposed algorithm successfully simulates the natural fading trajectory of the blemishes, showing a natural change in color.

Fréchet Inception Distance (FID) scores for the simulated images and the ground-truth images are calculated to quantitatively measure the quality of algorithms for skin blemish editing. The results are displayed in Table 5.1 and the visual comparison is shown in Figure 5.3.

For the FID scores, the proposed method achieved the lowest scores in the vast majority of cases, except for the 20% fading rate. In particular, the proposed method has less variation in FID scores compared to other baselines at different fading rates, which suggests that the proposed model is able to achieve robust, realistic skin blemish simulations.

Visual comparison more intuitively demonstrates the superiority of the proposed algorithm. The PS method, although straightforward, led to a loss of skin detail

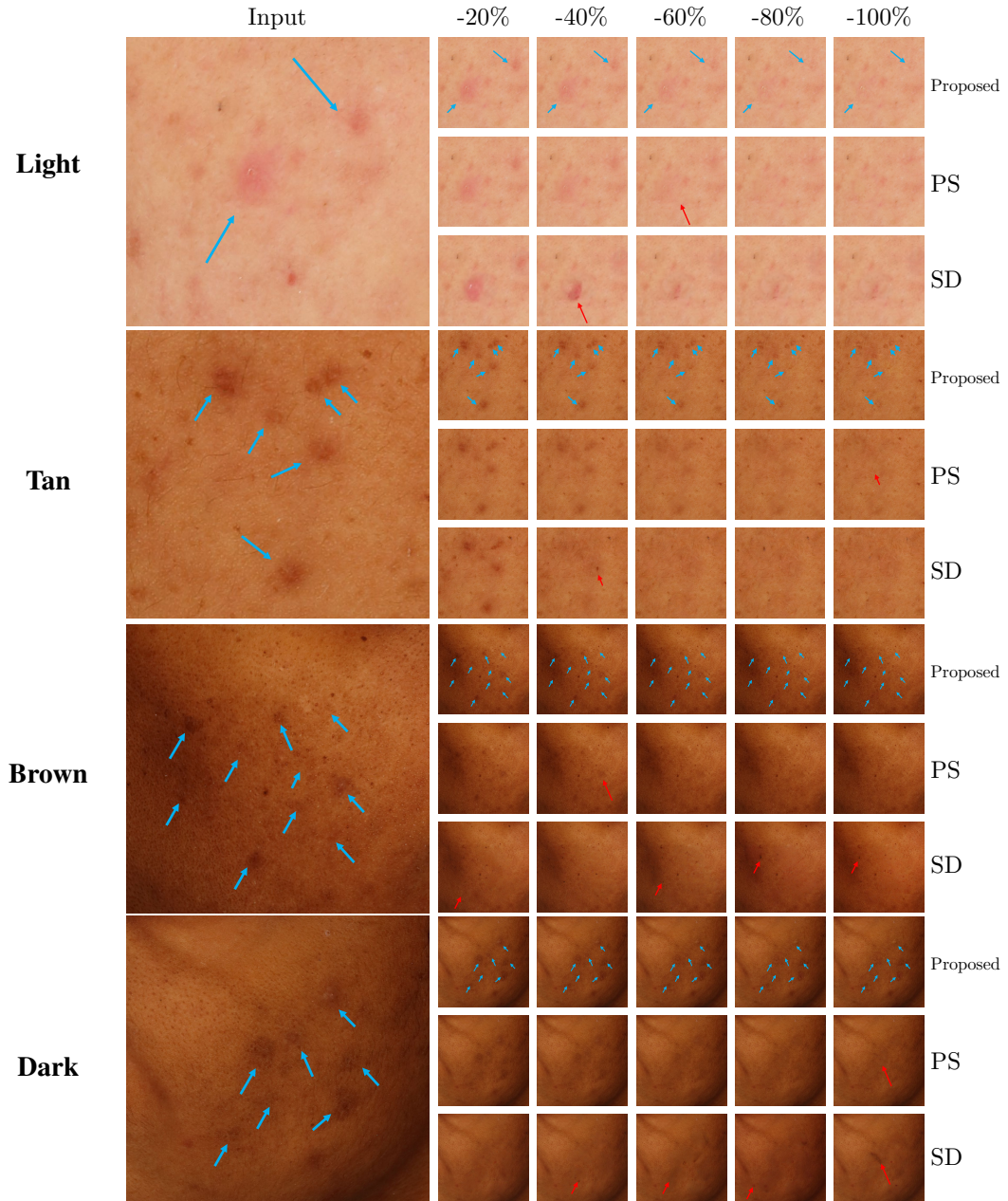


Figure 5.3: Comparison with baseline methods on various skin tones. The results of several blemish removal or modification methods are compared, including the proposed method (marked as Proposed), Adobe Photoshop [3] inpainting (marked as PS), and Stable Diffusion [4] inpainting (marked as SD). Arrows are manually added to highlight areas of interest. Note the red arrows where the PS produces over-smoothed skin patches and the SD produces visible artifacts. For darker skin tones, the SD method fails to simulate varying intermediate states of blemish removal, displaying similar results under different control intensities.

through simple interpolation, resulting in blurry patches. Conversely, the SD method generated some contextually coherent skin details while removing the

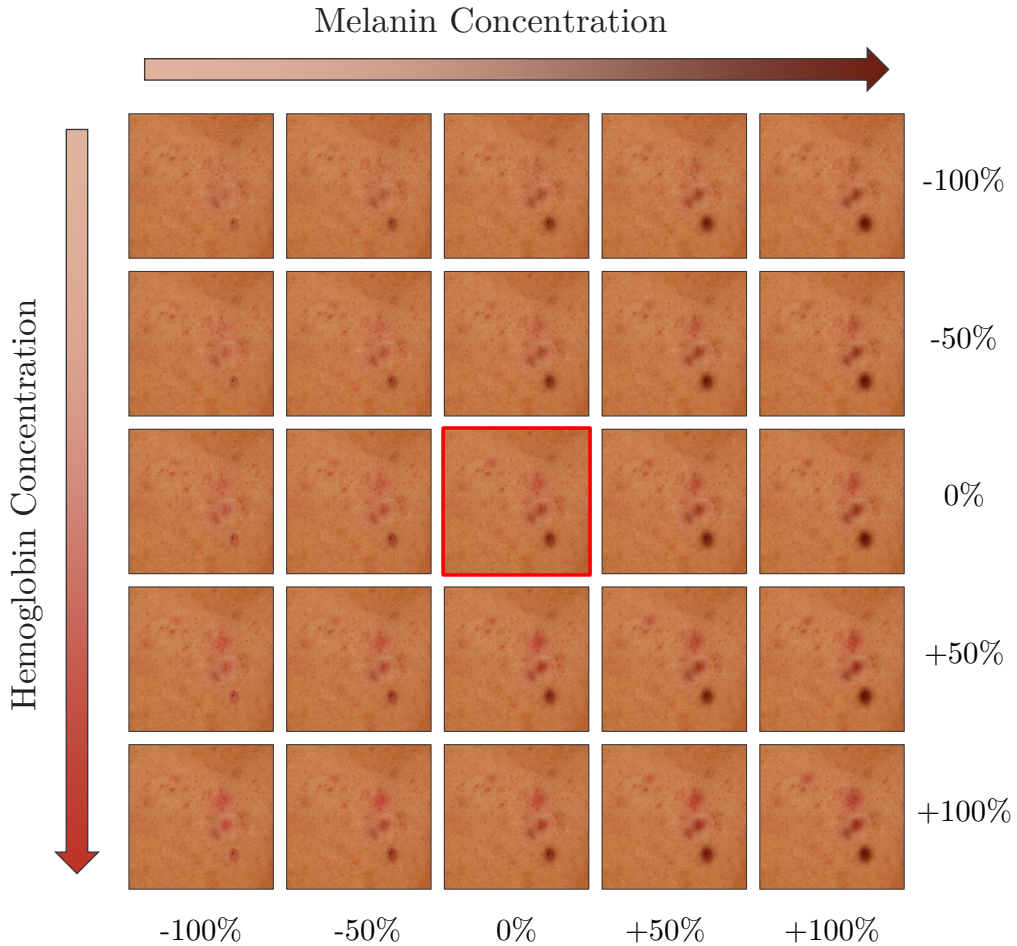


Figure 5.4: Matrix of different chromophore concentrations setting. The original image is marked by a red box. The proposed model fully decouples the major chromophores of human skin, enabling highly controllable blemishes editing.

blemishes, but its quality was limited. Specifically, at higher denoising ratios, the SD method produced noticeable artifacts, and the modified areas differed in color from the surrounding skin.

The proposed method not only closely aligns with the natural degradation process of real skin but also ensures that the modified blemishes match the underlying skin seamlessly. Unlike other techniques, this approach does not create artifacts or blurriness. It maintains skin details, including subtle textures such as hair and pores, leading to a natural appearance. This underlines the effective-

Table 5.2: Key Statistics and Score Distribution from the Image Perception Study

Score	Real Images (%)	Fake Images (%)
-2 (Definitely Fake)	4.11	5.37
-1 (Likely Fake)	20.46	25.22
0 (Indistinguishable)	24.20	26.56
1 (Likely Real)	38.28	32.80
2 (Definitely Real)	12.96	10.06
Average Score	0.35511	0.16956
Correctly Identified	51.23	30.59
Failed to Identify (including Indistinguishable)	48.77	69.42

ness of the proposed method in preserving the intricacy of skin texture while accomplishing realistic modifications.

5.3 Controllability

Controllability is key to user interaction with the proposed algorithm. A significant advantage of the proposed model is its high controllability, where users can freely adjust the parameters of the blemishes to precisely control its appearance. A changing matrix is plotted by adjusting the concentration control parameters of melanin and heamoglobin, as shown in Figure 5.4. The proposed method successfully decouples the concentrations of these two chromophores, allowing users to independently control their apparent features, thus flexibly simulating the change of blemishes under different conditions.

5.4 Perception Study

The objective of this study is to evaluate if the blemishes changing simulation is natural and believable. As shown in Figure 5.5b and Table 5.2, the altered images had a lower average score (0.16956 vs 0.35511), with only 30.6% cor-

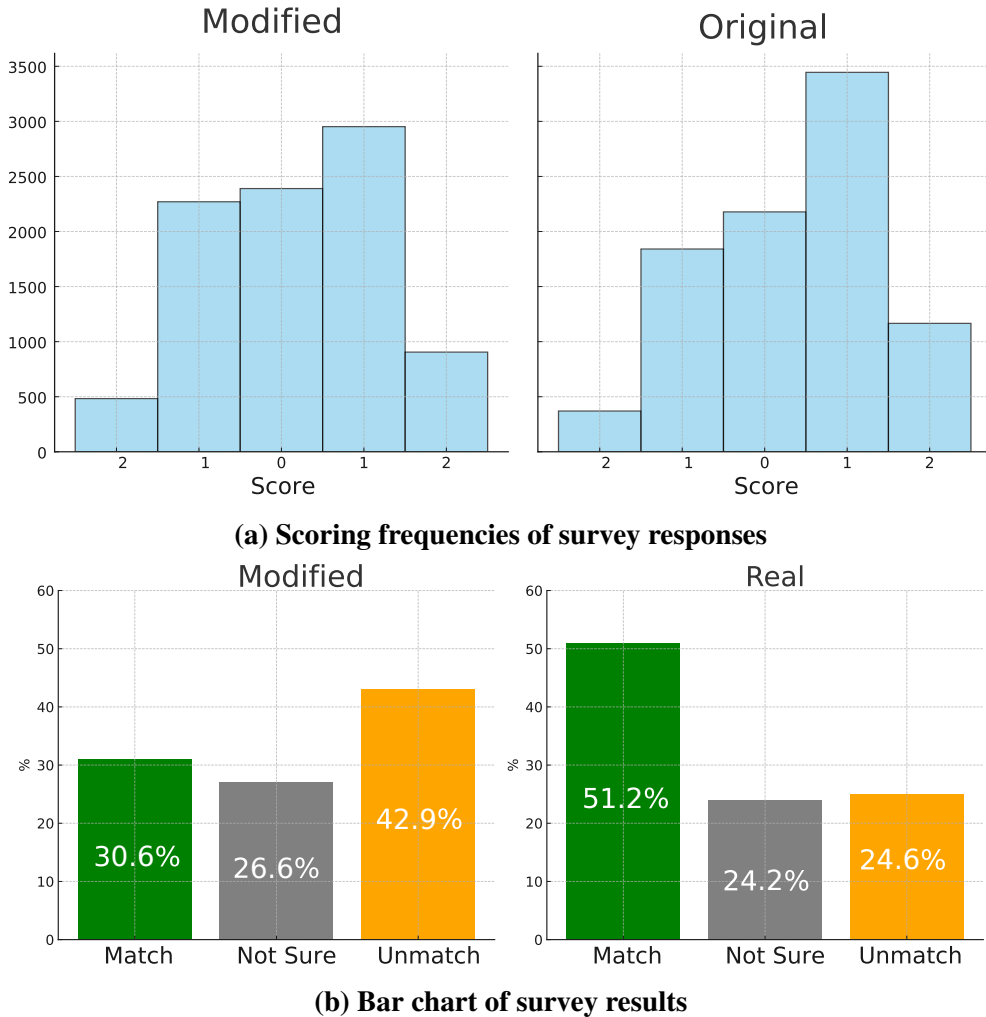


Figure 5.5: Panellists scored images from -2 to +2 to assess their confidence in considering the image as modified or not, with higher scores indicating that the user considered the image to be unmodified. Scoring frequencies are displayed in Figure 5.5a. The results of the survey are shown in Figure 5.5b. For the modified images, more people perceived them as unmodified or not sure. This suggests that the modifications are consistent with human perception and intuition.

rectly identifying the altered image vs 23.6% judging the real images as altered, and 26.6% not sure if it is or is not altered. This indicates that the effect of the proposed algorithm is superior, to the point where laypeople cannot readily discern traces of algorithmic alteration. The analysis revealed several key insights:

- **Score Distribution** The distribution of scores for both real and altered images showed a significant overlap, especially for scores 0 and 1, indicating

a level of ambiguity in distinguishing between real and simulated images.

- **Accuracy in Identification** Panellists correctly identified real images as real 51.23% of the time, whereas they correctly identified altered images only 30.59% of the time. This suggests a higher degree of realism in the simulated images.
- **Perception of Altered Images** Interestingly, a significant portion (42.86%) of the altered images were perceived as real, and when considering scores of 0 as indistinguishable, this figure rose to 69.41%. This underscores the effectiveness of the simulation in creating convincing images.

Chapter 6

Conclusion

In conclusion, the novel method presented in this research for simulating skin blemish changes marks a significant advancement in the realm of dermatological technology. By utilizing a physics-based model enriched with dermatological expertise, this approach successfully models facial skin blemishes, offering a highly controllable, natural, and authentic simulation of blemish changes over time. This system, demonstrating broad applicability across various skin tones and blemishes, stands out for its ability to achieve quality results without relying on extensive learning from large datasets, a common limitation in many learning-based image manipulation algorithms.

However, the method is not without its challenges. The requirement for manual selection of blemish areas points to a need for automation in future iterations, potentially through the integration of advanced detection algorithms. Additionally, the user study results suggest a necessity for refining the simulation's subtlety to enhance its realism further, particularly in the face of diverse human perceptions. The parameter settings, while effective within the scope of a controlled dataset, warrant additional testing in more variable, real-world scenarios to ensure broader applicability and reliability.

Looking ahead, this research opens up new pathways in the skincare industry, particularly in the development of skincare products. The potential for

this method to foster innovation and customization is significant, aligning well with the evolving demands of consumers seeking personalized skincare solutions. Moreover, the insights gained from this research could act as a catalyst for future interdisciplinary explorations, bridging the gap between computer vision and skin science. The development of more sophisticated, user-friendly, and versatile tools for skin blemish simulation and analysis could bring benefits for both consumer experience and dermatological research. As this field continues to evolve, the integration of machine vision, and image processing with dermatological knowledge will likely unveil new horizons in skincare and treatment, potentially transforming both daily skincare routines and professional dermatological practices.

References

- [1] Craig Donner and Henrik Wann Jensen. A Spectral BSSRDF for Shading Human Skin. In *Proceedings of the 17th Eurographics Conference on Rendering Techniques*, EGSR '06, page 409–417, Goslar, DEU, 2006. Eurographics Association.
- [2] K. S. Krishnapriya, Gabriella Pangelinan, Michael C. King, and Kevin W. Bowyer. Analysis of Manual and Automated Skin Tone Assignments. In *2022 IEEE/CVF Winter Conference on Applications of Computer Vision Workshops (WACVW)*, pages 429–438. IEEE.
- [3] Adobe Inc. Adobe photoshop.
- [4] Robin Rombach, Andreas Blattmann, Dominik Lorenz, Patrick Esser, and Björn Ommer. High-resolution image synthesis with latent diffusion models, 2021.
- [5] Ling Li, Bandara Dissanayake, Tatsuya Omotezako, Yunjie Zhong, Qing Zhang, Rizhao Cai, Qian Zheng, Dennis Sng, Weisi Lin, Yufei Wang, and Alex C. Kot. Evaluating the efficacy of skincare product: A realistic short-term facial pore simulation. *Electronic Imaging*, 35(7):276–1–276–1, 2023.
- [6] Lianxin Xie, Wen Xue, Zhen Xu, Si Wu, Zhiwen Yu, and Hau San Wong. Blemish-aware and Progressive Face Retouching with Limited Paired Data. In *2023 IEEE/CVF Conference on Computer Vision and Pattern Recognition (CVPR)*, pages 5599–5608. IEEE.

- [7] Tsung-Ying Lin, Yu-Ting Tsai, Tsung-Shian Huang, Wen-Chieh Lin, and Jung-Hong Chuang. Exemplar-based freckle retouching and skin tone adjustment. 78:54–63.
- [8] Alireza Shafaei, James J. Little, and Mark Schmidt. AutoRetouch: Automatic Professional Face Retouching. In *2021 IEEE Winter Conference on Applications of Computer Vision (WACV)*, pages 989–997. IEEE.
- [9] Ian J. Goodfellow, Jean Pouget-Abadie, Mehdi Mirza, Bing Xu, David Warde-Farley, Sherjil Ozair, Aaron Courville, and Yoshua Bengio. Generative Adversarial Networks.
- [10] Jonathan Ho, Ajay Jain, and Pieter Abbeel. Denoising diffusion probabilistic models. In Hugo Larochelle, Marc’Aurelio Ranzato, Raia Hadsell, Maria-Florina Balcan, and Hsuan-Tien Lin, editors, *Advances in Neural Information Processing Systems 33: Annual Conference on Neural Information Processing Systems 2020, NeurIPS 2020, December 6-12, 2020, virtual*, 2020.
- [11] Vincent Dumoulin, Jonathon Shlens, and Manjunath Kudlur. A learned representation for artistic style. In *5th International Conference on Learning Representations, ICLR 2017, Toulon, France, April 24-26, 2017, Conference Track Proceedings*. OpenReview.net, 2017.
- [12] Jun-Yan Zhu, Taesung Park, Phillip Isola, and Alexei A. Efros. Unpaired image-to-image translation using cycle-consistent adversarial networks. In *IEEE International Conference on Computer Vision, ICCV 2017, Venice, Italy, October 22-29, 2017*, pages 2242–2251. IEEE Computer Society, 2017.
- [13] Leon A. Gatys, Alexander S. Ecker, and Matthias Bethge. A neural algorithm of artistic style. *ArXiv preprint*, abs/1508.06576, 2015.
- [14] Norimichi Tsumura, Nobutoshi Ojima, Kayoko Sato, Mitsuhiro Shiraishi, Hideto Shimizu, Hirohide Nabeshima, Syuuichi Akazaki, Kimihiko Hori, and Yoichi Miyake. Image-based skin color and texture analysis/synthesis by extracting hemoglobin and melanin information in the skin. page 10.

- [15] Simon Alaluf, Derek Atkins, Karen Barrett, Margaret Blount, Nik Carter, and Alan Heath. Ethnic Variation in Melanin Content and Composition in Photoexposed and Photoprotected Human Skin. 15(2):112–118.
- [16] Motonori Doi and Shoji Tominaga. Spectral estimation of human skin color using the Kubelka-Munk theory. page 221.
- [17] R. Rox Anderson and John A. Parrish. The optics of human skin. *Journal of Investigative Dermatology*, 77(1):13–19, 1981.
- [18] Takanori Igarashi, Ko Nishino, and Shree K. Nayar. The appearance of human skin. 2005.
- [19] George Borshukov and J. P. Lewis. Realistic human face rendering for "the matrix reloaded". In *ACM SIGGRAPH 2005 Courses*, SIGGRAPH '05, page 13–es, New York, NY, USA, 2005. Association for Computing Machinery.
- [20] Brent Burley. Extending the disney brdf to a bsdf with integrated subsurface scattering. In *SIGGRAPH 2015 Course: Physically Based Shading in Theory and Practice*, 2015.
- [21] Jorge Jimenez, Károly Zsolnai, Adrian Jarabo, Christian Freude, Thomas Auzinger, Xian-Chun Wu, Javier von der Pahlen, Michael Wimmer, and Diego Gutierrez. Separable subsurface scattering. *Computer Graphics Forum*, 2015.
- [22] Magnus Wrenninge, Ryusuke Villemin, and Christophe Hery. Path traced subsurface scattering using anisotropic phase functions and non-exponential free flights. In *Tech. Rep.* Pixar Inc., 2017.
- [23] Matt Jen-Yuan Chiang, Peter Kutz, and Brent Burley. Practical and controllable subsurface scattering for production path tracing. In *ACM SIGGRAPH 2016 Talks*, pages 1–2. 2016.
- [24] Henrik Wann Jensen, Stephen R. Marschner, Marc Levoy, and Pat Hanrahan. *A Practical Model for Subsurface Light Transport*. Association for Computing Machinery, New York, NY, USA, 1 edition, 2023.

- [25] Eugene d’Eon, David Luebke, and Eric Enderton. Efficient rendering of human skin. In *Proceedings of the 18th Eurographics conference on Rendering Techniques*, pages 147–157, 2007.
- [26] Craig Donner and Henrik Wann Jensen. Light diffusion in multi-layered translucent materials. *ACM Trans. Graph.*, 24(3):1032–1039, 2005.
- [27] Diederik P. Kingma and Max Welling. Auto-encoding variational bayes. In Yoshua Bengio and Yann LeCun, editors, *2nd International Conference on Learning Representations, ICLR 2014, Banff, AB, Canada, April 14-16, 2014, Conference Track Proceedings*, 2014.
- [28] Tero Karras, Samuli Laine, and Timo Aila. A style-based generator architecture for generative adversarial networks. In *IEEE Conference on Computer Vision and Pattern Recognition, CVPR 2019, Long Beach, CA, USA, June 16-20, 2019*, pages 4401–4410. Computer Vision Foundation / IEEE, 2019.
- [29] Yujun Shen, Jinjin Gu, Xiaou Tang, and Bolei Zhou. Interpreting the latent space of gans for semantic face editing. In *2020 IEEE/CVF Conference on Computer Vision and Pattern Recognition, CVPR 2020, Seattle, WA, USA, June 13-19, 2020*, pages 9240–9249. IEEE, 2020.
- [30] Edward J. Hu, Yelong Shen, Phillip Wallis, Zeyuan Allen-Zhu, Yuanzhi Li, Shean Wang, Lu Wang, and Weizhu Chen. Lora: Low-rank adaptation of large language models. In *The Tenth International Conference on Learning Representations, ICLR 2022, Virtual Event, April 25-29, 2022*. OpenReview.net, 2022.
- [31] Lvmin Zhang and Maneesh Agrawala. Adding Conditional Control to Text-to-Image Diffusion Models. *ArXiv preprint*, abs/2302.05543, 2023.
- [32] Haoran Bai, Di Kang, Haoxian Zhang, Jinshan Pan, and Linchao Bao. Ffhq-uv: Normalized facial uv-texture dataset for 3d face reconstruction. In *IEEE Conference on Computer Vision and Pattern Recognition*, 2023.

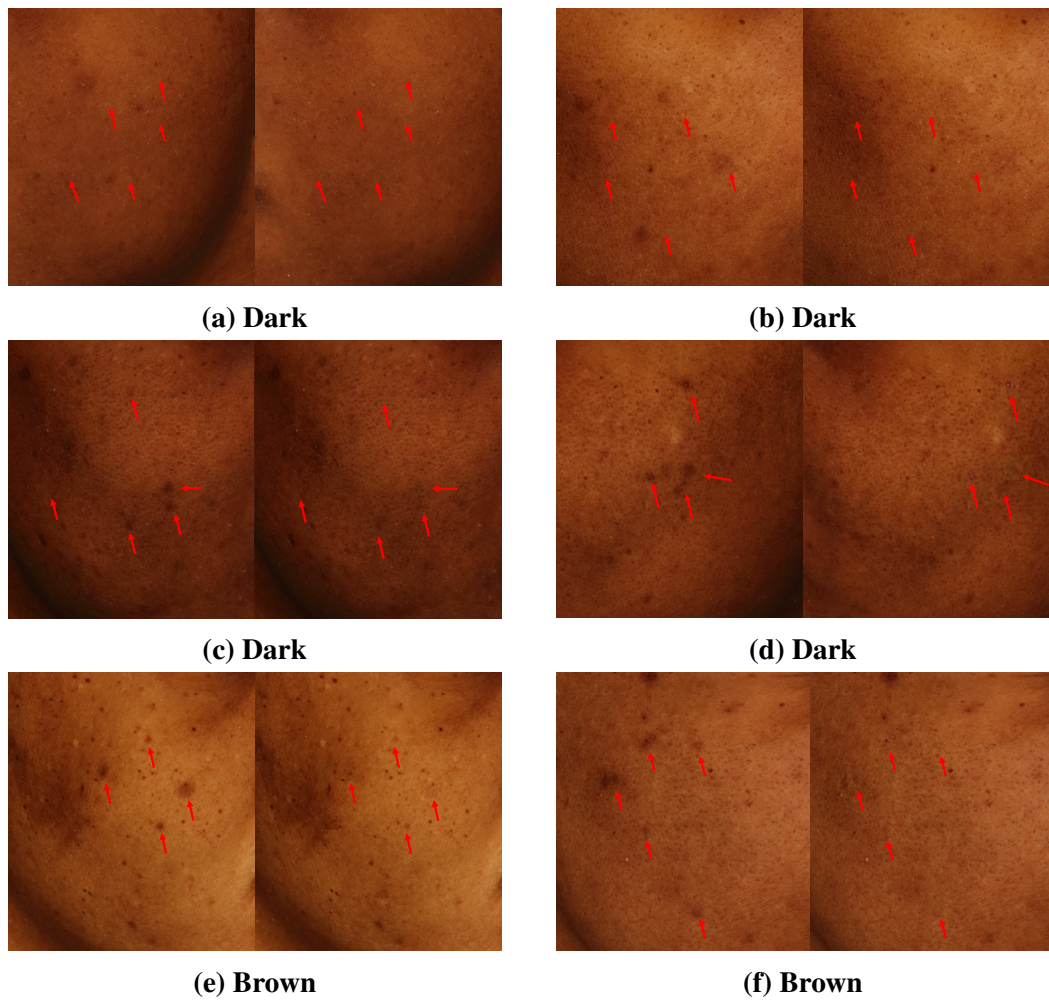
- [33] Kavita Behara, Ernest Bhero, and John Terhile Agee. Skin Lesion Synthesis and Classification Using an Improved DCGAN Classifier. 13(16):2635.
- [34] Marcelo Bertalmio, Andrea L Bertozzi, and Guillermo Sapiro. Navier-stokes, fluid dynamics, and image and video inpainting. In *Proceedings of the 2001 IEEE Computer Society Conference on Computer Vision and Pattern Recognition. CVPR 2001*, volume 1, pages I–I. IEEE, 2001.
- [35] Uri Lipowezky and Sarah Cahen. Automatic freckles detection and retouching. In *2008 IEEE 25th Convention of Electrical and Electronics Engineers in Israel*, pages 142–146.
- [36] Xin Liu, Lu Xie, Bineng Zhong, Jixiang Du, and Qinmu Peng. Automatic facial flaw detection and retouching via discriminative structure tensor. *IET Image Process.*, 11:1068–1076, 2017.
- [37] Sudha Velusamy, Rishabh Parihar, Raviprasad Kini, and Aniket Rege. Fab-Soft: Face Beautification via Dynamic Skin Smoothing, Guided Feathering, and Texture Restoration. In *2020 IEEE/CVF Conference on Computer Vision and Pattern Recognition Workshops (CVPRW)*, pages 2248–2256. IEEE.
- [38] Kaiming He, Jian Sun, and Xiaou Tang. Guided Image Filtering. In Kostas Daniilidis, Petros Maragos, and Nikos Paragios, editors, *Computer Vision – ECCV 2010*, Lecture Notes in Computer Science, pages 1–14. Springer.
- [39] Ji Liu, Shuai Li, Wenfeng Song, Liang Liu, Hong Qin, and Aimin Hao. Automatic Beautification for Group-Photo Facial Expressions Using Novel Bayesian GANs. In *Artificial Neural Networks and Machine Learning – ICANN 2018*, Lecture Notes in Computer Science, pages 760–770. Springer International Publishing.
- [40] Geunho Jung, Semin Kim, Jongha Lee, and Sangwook Yoo. Deep learning-based optical approach for skin analysis of melanin and hemoglobin distribution. 28(3):035001.

- [41] S.Elizabeth Whitmore and N.Joan Glavan Sago. Caliper-measured skin thickness is similar in white and black women. *Journal of the American Academy of Dermatology*, 42(1):76–79, 2000.
- [42] Norimichi Tsumura, Hideaki Haneishi, and Yoichi Miyake. Independent-component analysis of skin color image. *JOSA A*, 16(9):2169–2176, 1999.
- [43] A. Hyvärinen and E. Oja. Independent component analysis: algorithms and applications. *Neural Networks*, 13(4):411–430, 2000.
- [44] F. Pedregosa, G. Varoquaux, A. Gramfort, V. Michel, B. Thirion, O. Grisel, M. Blondel, P. Prettenhofer, R. Weiss, V. Dubourg, J. Vanderplas, A. Passos, D. Cournapeau, M. Brucher, M. Perrot, and E. Duchesnay. Scikit-learn: Machine learning in Python. *Journal of Machine Learning Research*, 12:2825–2830, 2011.
- [45] Jorge J. Moré. The levenberg-marquardt algorithm: Implementation and theory. In G. A. Watson, editor, *Numerical Analysis*, pages 105–116, Berlin, Heidelberg, 1978. Springer Berlin Heidelberg.
- [46] Matthew Newville, Till Stensitzki, Daniel B. Allen, and Antonino Ingargiola. LMFIT: Non-Linear Least-Square Minimization and Curve-Fitting for Python, 2014.
- [47] Christian Szegedy, Vincent Vanhoucke, Sergey Ioffe, Jonathon Shlens, and Zbigniew Wojna. Rethinking the inception architecture for computer vision. In *2016 IEEE Conference on Computer Vision and Pattern Recognition, CVPR 2016, Las Vegas, NV, USA, June 27-30, 2016*, pages 2818–2826. IEEE Computer Society, 2016.

Appendix A

Simulation on Various Skin Tones

The proposed model's performance on different skin tones is displayed here. In each set, the left image is the input, and the right image is the output. Arrows indicate the pigmentation or acne of interest, selected by the panellists. These chosen skin blemishes are completely removed by the proposed model. Zoom in for a better view.





(g) Brown



(h) Brown



(i) Tan



(j) Tan



(k) Intermediate



(l) Intermediate



(m) Light



(n) Light



(o) Light



(p) Light